Spontaneous Ca2+ transients in mouse microglia

Korvers, L. and de Andrade Costa, A. and Mersch, M. and Matyash, V. and Kettenmann, H. and Semtner, M.

Cell Calcium
2016 DEC ; 60(6): 396-406
2016 SEP 22 (first published online)
doi: 10.1016/j.ceca.2016.09.004

Publisher: Elsevier

Spontaneous Ca^{2+} transients in mouse microglia

Laura Korvers[a], Amanda de Andrade Costa[a], Martin Mersch[a], Vitali Matyash[a], Helmut Kettenmann[a*] and Marcus Semtner[a*]

[a] Max-Delbrueck-Centrum for Molecular Medicine (MDC) in the Helmholtz Association, Cellular Neurosciences, Robert-Roessle-Str. 10, 13125 Berlin, Germany

[*] Equal Contribution

Corresponding author:

Marcus Semtner

Max-Delbrueck-Centrum for Molecular Medicine in the Helmholtz Association (MDC)

Cellular Neurosciences

Robert-Roessle-Str. 10

13092 Berlin, Germany

marcus.semtner@mdc-berlin.de

Abstract

Microglia are the resident immune cells in the central nervous system and many of their physiological functions are known to be linked to intracellular calcium (Ca^{2+}) signaling. Here we show that isolated and purified mouse microglia – either freshly or cultured - display spontaneous and transient Ca^{2+} elevations lasting for around ten to twenty seconds and occurring at frequencies of around five to ten events per hour and cell. The events were absent after depletion of internal Ca^{2+} stores, by phospholipase C (PLC) inhibition or blockade of inositol-1,4,5 trisphosphate receptors (IP_3Rs), but not by removal of extracellular Ca^{2+}, indicating that Ca^{2+} is released from endoplasmic reticulum intracellular stores. We furthermore provide evidence that autocrine ATP release and subsequent activation of purinergic P2Y receptors is not the trigger for these events. Spontaneous Ca^{2+} transients did also occur after stimulation with Lipopolysaccharide (LPS) and in glioma-associated microglia, but their kinetics differed from control conditions. We hypothesize that spontaneous Ca^{2+} transients reflect aspects of cellular homeostasis that are linked to regular and patho-physiological functions of microglia.

Key words

microglia, spontaneous, calcium, IP_3 receptor, endoplasmic reticulum, purinergic receptors

Abbreviations

ATP, adenosine triphosphate; Ca^{2+},calcium ions; $[Ca^{2+}]_I$ intracellular calcium concentration; CPA, cyclopiazonic acid; ER, endoplasmic reticulum; GAM, glioma-associated microglia; hGAM, human GAM; IP_3, inositol-1,4,5-trisphosphate; IP_3R, IP_3 receptor; LPA, lysophosphatic acid; LPS, lipopolysaccharide; mGAM, mouse GAM; P2XR, P2X receptor; P2YR, P2Y receptor; PLC, phospholipase C; PMCA, plasma membrane Ca^{2+} ATPase; RyR, ryanodine receptor; SERCA, sarco-/endoplasmatic Ca^{2+} ATPase; UDP, uridine diphosphate

1. Introduction

Microglia are the resident immune cells in the central nervous system (CNS). In the healthy brain, they are characterized by a ramified morphology, and monitor their surroundings for environmental changes [1-3]. Under disease conditions such as inflammation or ischemia, microglia change into an activated state which is characterized by morphological transformation into an amoeboid form [for reviews see 4, 5] as well as by functional changes which include migration, proliferation, the release of several cytokines, and phagocytosis of damaged cells or debris [6-9]. Many features of microglia were previously shown to be linked to purinergic signaling and intracellular calcium (Ca^{2+}) pathways. Thus, microglial migration towards damaged, ATP-releasing sites is mediated by $P2Y_{12}$ receptors which are linked to phospholipase C (PLC) signaling and Inositol-1,4,5-trisphoisphate (IP_3) -mediated cytosolic Ca^{2+} elevations [6]. Like in many other cell types, proliferation of microglia depends on intracellular Ca^{2+} signaling, and microglial proliferation was furthermore reported to be induced or increased by thrombin or LPA - both ligands linked to PLC signaling [10, 11, for a review see 12]. Furthermore, phagocytic activity of microglia is mediated by UDP and the G_q protein coupled receptor $P2Y_6$ [2], and further regulated by store-operated Ca^{2+} entry [13, 14].

The major elements of intracellular Ca^{2+} signaling are almost identical for all cell types [15], and are therefore also valid for microglia. The relatively low cytosolic Ca^{2+} concentration ($[Ca^{2+}]_i$) of most healthy and resting cells - usually being in the range between 50-100 nM- is maintained by the action of Ca^{2+} ATPases located in the endoplasmic reticulum (ER) and in the plasma membrane (SERCA and PMCA, respectively). Since the ER luminal and the extracellular Ca^{2+} concentrations are much higher than $[Ca^{2+}]_i$, cytosolic Ca^{2+} levels elevate whenever Ca^{2+}-permeable ion channels in the ER membrane or plasma membrane are opened. $[Ca^{2+}]_i$ of cultured human microglia was previously determined to be around 66 nM [16]. In addition to ligand-evoked intracellular Ca^{2+} elevations, Hegg et al. also described the appearance of spontaneous microglial Ca^{2+} elevations. These elevations were later attributed to an ATP- and $P2X_7$-dependent astrocyte-microglia interaction [17]. More recently, spontaneous calcium transients in microglia were also reported *in vivo* and *in situ* [18, 19] but in contrast, the signaling mechanism was dependent on intracellular Ca^{2+} stores and independent from astrocytic or neuronal Ca^{2+} waves. The authors concluded that the spontaneous Ca^{2+} transients may be triggered by neuronal, damage-induced ATP release.

In the present study, we show that spontaneous Ca^{2+} transients do also occur in various isolated microglia preparations which are devoid of any other cell type. From their appearance, kinetics and pharmacology, the events described here resemble all characteristics of those

transients that were previously described in vivo [18, 19]. Since there were no other cell types in our preparations, and since the spontaneous Ca^{2+} transients were not dependent on the microglia culturing density, we suggest that they originate from intrinsic microglial signaling. This in turn indicates that spontaneous Ca^{2+} transients may reflect aspects of cellular homeostasis. We furthermore found that the appearance and kinetics of spontaneous Ca^{2+} transients of glioma-associated and in LPS-stimulated microglia are changed in comparison to control microglia, indicating that they may be also linked to patho-physiological functions of microglia.

2. Materials and methods

2.1. Solutions and chemicals

All chemicals were ordered from Sigma Aldrich (Darmstadt, Germany), unless stated otherwise. During life cell calcium imaging, cells were kept in standard buffer (in mM: 150 NaCl, 5.4 KCl, 0.98 $MgCl_2$ * 6 H_2O, 1.97 $CaCl_2$ * 2 H_2O, 6.08 HEPES, 9.9 glucose), unless otherwise specified. In experiments where extracellular Ca^{2+} was omitted from the buffer, $CaCl_2$ * 2 H_2O from the standard buffer was replaced for a total of 2 mM $MgCl_2$ * 6 H_2O and supplemented with 0.5 mM EGTA. The following substances were prepared by dissolving them in standard buffer and 0.1% DMSO: 2.5 µM thapsigargin (Santa Cruz Biotechnology, Dallas, Texas, USA), 20 µM U73122 (Tocris Bioscience, Bristol, UK), 20 µM ryanodine (Tocris Bioscience), 5 µM carbonyl cyanide – *p* – trifluoromethoxyphenylhydrazone (FCCP) (Abcam, Cambridge, UK), 20 µM CGP37157 (Tocris Bioscience). 20 µM cyclopiazonic acid (CPA) was dissolved in 0.1% chloroform. Due to the high osmolarity of caffeine (10 mM), NaCl was reduced to 140 mM in HEPES buffer and slightly heated (37°C) to dissolve caffeine. For acute LPS application, 100 ng/ml LPS was directly dissolved in standard buffer. For chronic application, 100 ng/ml LPS was applied to the culturing medium (DMEM) and incubated for 12 or 36 h at 37 °C. The following substances were prepared by dissolving them in standard buffer: 1 mM ATP, 50 µM ruthenium red (Abcam), 50 µM carbenoxolone, 50 µM reactive blue, 100 µM PPADS (pyridoxalphosphate-6-azophenyl-2',4'-disulfonic acid), 100 µM suramin and 5 µM MRS2578. 500 nM bafilomycin was added to the culturing medium and incubated for 12 h at 37 °C.

2.2. Generation of intracranial mouse gliomas

C57BL/6 (8-10 weeks old) mice were handled according to governmental (LaGeSo) and internal (MDC) rules and regulations. Briefly, after anesthetization, the mouse head was placed onto a stereotactic frame (David Kopf Instruments, Tujunga, California, USA). Through a midline incision, a burr hole was drilled at 1 mm anterior and 2 mm lateral to the bregma. Canals were created by inserting a 1 µl Hamilton syringe 4 mm ventral from dura mater and retracted to a depth of 3 mm from the dural surface. Total of 1 µl ($2x10^4$cells/µl) GL261 cell suspension was slowly injected. The needle was then slowly taken out from the injection canal and skin was sutured with a surgical sewing cone (Johnson & Johnson, New Brunswick, New Jersey, USA). Mice were monitored daily for the first two weeks and twice a day starting from day 14 post-injection for symptoms of tumor development (lethargy, hydrocephalus and head tilting).

2.3. Preparation of acutely isolated microglia

To obtain glioma-associated macrophages/microglia, GL261-implanted mice were sacrificed 20 days post-injection, tumour-bearing and control mice were euthanized by i.p. injection of an overdose of pentobarbital-sodium (Narcoren, Pharmazeutischen Handelsgesellschaft, Garbsen-Berenbostel, Germany) and perfused using an ice-cold PBS solution. The brains were extracted and stored in ice-cold HBSS (Gibco-Invitrogen, Darmstadt, Germany). For naïve mouse brains, the olfactory bulbs and the cerebellum were cut by a scalpel and discarded. The rest of the tissue was used for dissociation. In tumor-bearing mouse brains, only the visible tumor area around the injection site was used. Microglia was freshly isolated and purified for calcium imaging using magnetic activated cell sorting (MACS). Microglia were isolated from cell suspensions using magnetic CD11b microbeads™ from Miltenyi Biotech (Bergisch Gladbach, Germany), according to the manufacturer's instructions. The tumours were dissociated using the Miltenyi Biotec Neural Tissue Dissociation Kit (Trypsin), as previously described [20] (. After dissociation using a glass Pasteur pipette, the suspension was passed through a 40 µm cell strainer followed by centrifugation for 5 minutes at 500g and 4^{o}C to obtain a single cell suspension. The cell suspension was then incubated for 15 minutes with Miltenyi Biotec myelin removal beads, followed by magnetic separation using LargeScale columns (Miltenyi Biotec), with 2 columns used per tumour. In naïve mice, the brain cells were mechanically dissociated with a syringe plunger against a 70 µM cell strainer and the myelin removal was carried out using a protocol described elsewhere [21]. Briefly, the resulting brain cell suspension was mixed with a total of 10 ml of a 22% Percoll (Th.Geyer, Renningen, Germany) solution and a layer of 2 ml cold PBS (Gibco-Invitrogen) was added on top. Centrifugation at 950 g with slow acceleration and without breaks created a gradient that separated the cell pellet on the bottom of the tube from the myelin which was carefully aspirated [20] . Following myelin removal, the myelin free flow-through was incubated with CD11b beads in MACS buffer (PBS supplemented with 0.5% BSA and 2 mM EDTA) for 20 minutes, and the cell suspension was applied to a MediumScale column (Miltenyi Biotec) and washed three times with MACS buffer. Labelled CD11b^{+} cells within the column were then flushed out and plated onto glass coverslips, followed by 15 minutes incubation in Dulbecco's Modified Eagle's Medium (DMEM) (Gibco-Invitrogen) medium to allow adherence.

2.4. Primary neonatal cultured microglia

For preparation of neonatal cultured microglia, P0 – P3 mice were used. After extraction of the brains, meninges and cerebellum were removed and put on ice with HBSS. The dissected brains were washed 3 times before adding trypsin (10 mg/ml) and DNAse (0.5 mg/ml) in PBS.

After 2-3 min of incubation with this solution, the reaction was blocked by adding DMEM containing 10% FCS. After removal of the medium, 0.2 mg DNAse was added and the cells were mechanically dissociated. This step was repeated before centrifuging the cells 10 min at 800 rpm at 4 C. The supernatant was discarded. The pellet was resuspended in DMEM (2 brains/ml) and plated (2 brains/flask) in Poly – L - Lysine coated flasks. After 24-48 h of incubation, the cultures were washed 3 times with PBS and allowed to grow until confluent in DMEM (5 days). After this incubation period, medium was replacedby DMEM with 33% L929 conditioned medium. After 2 days, cells were harvested by shaking them for 30 min at 100 – 110 rpm. The supernatant was centrifuged for 10 min at 800 rpm at 4°C. The cells were counted and plated onto coverslips (1.5×10^5 cells/ coverslip). This procedure could be repeated for 2 times with 2 days interval.

2.5. Primary adult cultured microglia

For preparation of adult cultured microglia, 8 – 12 weeks old animals were used. During dissection of the cortex, the brain was kept in HBSS. The meninges were removed and the remaining cortex was cut in dices. The tissue was washed 2x with HBSS and incubated with trypsin (10 mg/ml) and DNAse (0.5 mg/ml) for 4 min at room temperature. After the incubation, cells were mechanically dissociated and centrifuged for 10 min at 4°C with 800 rpm in DMEM containing 10% FCS and 1% penicillin, streptomycin and glutamine (PSG). The remaining pellet was resuspended in 2 ml medium and filtered with a 40 µm filter (Falcon 9040739, Thermo Fisher Scientific). The cells were seeded on a chlodronate-treated pre-culture and incubated at 37°C. After 3 days, the cultures were washed with PBS and incubated with DMEM supplemented with 10% FCS and 1% PSG. After 1 week, the medium was replaced by 10 ml DMEM with 5 ml L929 conditioned medium. After 1 week, the cells were harvested by shaking the cultures for 30 min at 100 – 110 rpm. The supernatant was centrifuged for 10 min at 800 rpm at 4°C. The cells were counted and plated onto coverslips with a diameter of 1,3 cm. Cell density was 1.5×10^5 cells/coverslip (1.12×10^5 cells/cm^2) if not state otherwise. This procedure could be repeated for 2 times with 7 days interval.

2.6. Preparation of freshly isolated human glioma-associated microglia/macrophages

The work with resected human gliomas was performed according to the rules by the Ethical Committee (UKSH, B 307/15 “Investigating the interaction of high-grade gliomas and microglia cells”).To obtain glioma-associated macrophages/microglia, resected human glioma tissue was provided by the Department of Neurosurgery Universitätsklinikum Schleswig-Holstein (Kiel,

Germany) and stored in ice-cold HBSS (Gibco-Invitrogen, Darmstadt, Germany). Human glioma associated-microglia/macrophages were freshly isolated and purified for Ca^{2+} imaging using magnetic activated cell sorting (MACS). The human glioma tissue was manually dissociated using the Miltenyi Biotec Neural Tissue Dissociation Kit (Trypsin), according to the manufacturer's instructions. The erythrocytes were depleted using an ammonium chloride buffer. Myelin was removed using Miltenyi Biotec´s Myelin Removal Kit, also according to the manufacturer´s instructions. Human Glioma associated Macrophages/Microglia were isolated from the cell suspension using magnetic CD11b MicroBeads from Miltenyi Biotech (Bergisch Gladbach, Germany), according to the manufacturer's instructions and plated onto glass coverslips, by plating 15- $20x10^3$ cells in a 5 µl drop of culture medium composed of Dulbecco's Modified Eagle's Medium (DMEM) (Gibco-Invitrogen) with 200 mM glutamine, 50 units/ml penicillin and 50 µg/ml streptomycin. Cells were incubated subsequently for 15 min at 37°C with a 5% CO_2 in a 24 well plate to allow adherence. Finally, 500µl of culture medium were added and calcium imaging was performed as fast as possible.

2.7. Polymerase Chain Reaction

RNA was isolated using the NucleoSpin RNA kit according to the manufactures instructions (Macherey – Nagel, Düren, Germany). In brief, the cells were shaken off from the astrocytic monolayer and washed with PBS. Next, the cells were lysed and cleared. The RNA was bound to a filter column and washed. The purified RNA was dissolved in 60 µl RNAse-free H_2O. Concentration and purity of the RNA was determined with the Nanodrop 8000 Spectrophotometer (Thermo Fisher Scientific, Waltham, MA USA). 150 ng RNA, 0.56 mM dNTP (Invitrogen) and 281 µg/µl OligoDT (Invitrogen) was incubated at 65°C for 5 min and 1x first strand buffer (Invitrogen), 11 mM DTT and 40 U RNAse out (Invitrogen) was added to the mixture. Solution was incubated for 2 min at 42°C before adding 200 U SS RT enzyme (Invitrogen). The mixture was incubated for 50 min at 42°C. The reaction was terminated by incubating the solution 15 min at 70°C. 1 ng cDNA was mixed with 1x GoTaq Green Mastermix (Promega Corporation, Madison, WI, USA) and 0.5 ng/µl primer mix. A T3000 thermocycler (Biometra, Göttingen, Germany) was set to 3 min at 94°C, followed by 35 s at 60°C, 35 s at annealing temperature and 30 s at 72°C which was repeated for 35 times. The program ended with 10 min at 71°C. The annealing temperature was set at 60 °C for the IP_3R primers and at 59°C for the RyR primers (Biotex Laboratory, Houston, Texas, for sequences). Samples ran on a 2% agarose gel for analysis. Gene-specific primers were designed using the NCBI Primer BLAST tool [22], and had the following sequences: ITPR1: CGTTTTGAGTTTGAAGGCGTTT,

CATCTTGCGCCAATTCCCG; ITPR2: CCTCGCCTACCACATCACC, TCACCACTCTCACTATGTCGT; ITPR3: GGGCGCAGAACAACGAGAT, GAAGTTTTGCAGGTCACGGTT; RYR1: CCTTGGCTTCAGCCTTCTG, TCTGGGAGAGACACCTGTTGT; RYR2: ATGGCTTTAAGGCACAGCG, CAGAGCCCGAATCATCCAGC; RYR3: CTGAGCTGGTCCACTTTGTAAA, GAGGTCACCTAATCCCACTTCA.

2.8. Ca^{2+} imaging

Cells were incubated with 5 µM Fluo-4/AM (Thermo Fisher Scientific), 0.1% DMSO, 0.02% w/v pluronic F-127 (Thermo Fisher Scientific) in standard buffer for 40 min at room temperature. Prior to the recordings, cells were washed for 10-15 min in standard buffer. Fluorescence signals were recorded at excitation and emission wavelengths of 488 nm and 510 nm, respectively, using a Polychrome IV monochromator, a Till Imago camera (FEI, Gräfelfing, Germany) and CamWare software (PCO AG, Kelheim, Germany). During recording, cells were superfused with standard buffer using a peristaltic pump (4 ml/min,). Pictures were taken with a frequency of 2 frames/s and an exposure time of 50 ms using a 20x water immersion objective (Olympus, Tokyo, Japan).

2.9. Data analysis

Videos were analyzed using ImageJ 1.48g (Wayne Rasband, National Institutes of Health, USA). The integrated density was exported from each region of interest and further analyzed with a custom made algorithm in Igor Pro 6.3 (WaveMetrics, Lake Oswego, USA). All data are given as mean ± S.E.M. Significance was tested by one-way ANOVA and post-hoc Tukey tests. Significance is given by: n.s., $p > 0.05$; *, $p < 0.05$; **, $p < 0.01$; ***, $p < 0.001$.

3. Results

3.1 Spontaneous Ca^{2+} transients occur in adult freshly isolated and cultured microglia

We isolated and purified microglia from P60-P70 mouse brain, loaded the cells with the Ca^{2+}-sensitive dye Fluo4-AM® and performed Ca^{2+} imaging experiments in order to study spontaneous Ca^{2+} transients (Fig. 1A, Suppl. Fig. 1 and 2). To test for the viability of the cells, 1 mM ATP was applied at the end of each experiment. In 86.0 ± 3.8% of the freshly-isolated microglia, an ATP-evoked Ca^{2+} response was recorded. Spontaneous cytosolic Ca^{2+} transients occurred during a recording time of 12.5 min (n = 233 cells/12 coverslips, 5 animals) in 11.9 ± 3.7% of all analyzed freshly-isolated microglia at a calculated frequency of 1.9 ± 0.5 per cell and hour (Fig. 1E). Rise (16.0 ± 1.8 s) and decay times (34.4 ± 5.8 s) were close to those reported previously *in vivo* (Fig. 1F).

We tested whether cultured microglia could represent a model to analyze spontaneous Ca^{2+} transients *in vitro* (Fig. 1B and Suppl. Fig. 2). ATP application at the end of each experiment on cultured microglia prepared from P60-P70 mice (3 animals, 15 coverslips, 335 cells) led to Ca^{2+} responses in 98.3 ± 1.2% of cultured microglia. This was significantly higher (p = 0.0083) than in freshly isolated preparations, indicating that the latter contains damaged cells. Like in the acute preparation, spontaneous Ca^{2+} transients occurred also in cultured microglia at similar frequencies (2.5 ± 0.4 per cell and hour; p = 0.0854 compared to freshly-isolated; Fig. 1E). However, the decay kinetics of cultured microglia were significantly faster (17.2 ± 1.1 s, p = 0.0037) whereas there was no difference in rise times (15.4 ± 1.1 s, p = 0.6039; Fig. 1F). Cultured microglia from neonatal mice (P0-P3, n = 4205 cells, 67 coverslips, 18 culture preparations) displayed spontaneous Ca^{2+} transients which were similar to adult (12.5 ± 0.4 s, p = 0.3734 and 13.4 ± 0.4 s, p = 0.18 for rise and decay times, respectively, Fig. 1C, F) but occurred at higher frequencies (7.9 ± 0.7 per cell and hour, n = 67, p 0.0302 compared to adult; Fig. 1E). When cultured neonatal microglia were seeded at a lower density ($0.02x10^5$ cells/cm^2; Fig. 1D,E,F, n = 58 cells, 7 coverslips, 2 culture preparations), the frequency (5.9 ± 1.8 per cell and hour; p = 0.3591 compared to high density; Fig. 1E) and kinetics (10.7 ± 1.4 s, p = 0.2750 and 14.0 ± 2.5 s, p = 0.8098 for rise and decay times, respectively, Fig.1F) of the spontaneous Ca^{2+} transients remained nearly unchanged compared to the standard, high-density culture ($1.12x10^5$ cells/cm^2).

Taken together, these data show that spontaneous Ca^{2+} elevations are a generic feature of microglia isolated from mouse brain. The frequency of occurrence in neonatal microglia is higher than in adult microglia but their basic parameters (rise time, decay time) are in a

comparable range. We henceforth used neonatal microglia to investigate the mechanisms underlying microglial spontaneous Ca^{2+} transients in more detail.

3.2. Spontaneous Ca^{2+} transients emerge from intracellular stores

As reported for many other cell types, microglial cytosolic Ca^{2+} elevations may either occur due to Ca^{2+} entry from the extracellular space or by release from intracellular Ca^{2+} stores [for a review see 15]. To distinguish between these two possibilities, we investigated neonatal microglia in 0 mM Ca^{2+}/ 10 mM EGTA, thus, abolishing Ca^{2+} entry through the plasma membrane. As shown in Fig. 2B, the Ca^{2+} transients were still present under these conditions (Fig. 2A and E). However, the percentage of 'active' microglia (23.5 ± 4.2%, n = 25 coverslips/1003 cells, 4 culture preparations, p = 0.0020) was significantly decreased compared to control conditions (49.6 ± 2.5%, n = 67); and the frequencies were lower (2.9 ± 0.7 events/h and cell, p = 0.0037), indicating that extracellular Ca^{2+} has modulary effects on spontaneous Ca^{2+} transients. The rise and decay times of spontaneous Ca^{2+} transients did also change under Ca^{2+}-free conditions and appeared to be slightly faster (10.8 ± 0.5 s, p = 0.0093 and 11.5 ± 0.7 s, p = 0.0240, respectively). To further investigate the impact of Ca^{2+} entry from the extracellular space, we studied spontaneous Ca^{2+} transients in the presence of 50 µM ruthenium red, which antagonizes several Ca^{2+}-permeable channels including voltage-dependent calcium channels and TRP channels. However, in line with the small effects of Ca^{2+} withdrawal from extracellular medium, application of ruthenium red did not influence the occurrence of spontaneous Ca^{2+} transients (5.3 ± 1.0 events/h and cell, n=254 cells, 5 coverslips, 2 culture preparations; p = 0.3445 compared to control, Suppl. Fig. 3C,D). To test for a possible contribution of P2X receptors on microglial Ca^{2+} transients, we applied 100 µM PPADS which antagonizes the P2X subtypes 1-3,5 and 7 [23]. The frequency was drastically increased (n = 464 cells, 11 coverslips, 1 culture preparation) under these conditions (Fig. 4B,E; see section 3.4.), indicating that the spontaneous transients do not arise from Ca^{2+} entry through P2X receptors, but there must be at least a modulatory mechanism based on these ion channels.

Our data indicate that spontaneous Ca^{2+} transients in microglia arise rather from intracellular sources than from the extracellular space. We therefore examined the impact of manipulations of intracellular Ca^{2+} stores in the next series of experiments. Intriguingly, spontaneous microglial Ca^{2+} transients disappeared completely when the endoplasmic reticulum (ER) Ca^{2+} stores were depleted by blockers of SERCA (Fig.2 C and D). For both substances tested (thapsigargin, n = 786 cells, 11 coverslips, 6 culture preparations or CPA n = 766 cells, 10 coverslips. 3 culture

preparations), wash-in was followed by a large and transient increase in intracellular Ca^{2+} that reflects the leakage of Ca^{2+} from the ER into the cytosol, an effect which is known from previous publications [e.g. 14]. After addition and in the presence of 2.5 µM thapsigargin or in the presence of 20 µM CPA, none of the microglia displayed spontaneous Ca^{2+} transients (, $p < 0.0001$ and $n = 10$, $p < 0.0001$ compared to control, respectively), indicating that the ER is the primary Ca^{2+} source of these events. Interestingly, the application of 5 µM FCCP (carbonyl – cyanide – *p* – trifluoromethoxyphenylhydrazone), an uncoupler of oxidative phosphorylation in mitochondria, also abolished the generation of spontaneous Ca^{2+} transients in microglia (Suppl. Fig. 3A, n = 571 cells, 13 coverslips, 3 preparations). However, uncoupling the mitochondrial proton gradient and the associated loss of ATP synthesis will inevitably lead to the inhibition of all ATPases in the cell, including SERCA. Indeed, like with thapsigargin or CPA, a transient increase in intracellular Ca^{2+} was observed immediately after FCCP wash-in, possibly to a secondary depletion of ER Ca^{2+} stores by inhibition of SERCA. In order to test mitochondria as a possible further Ca^{2+} source of the transients, the mitochondrial Na^+/Ca^{2+} exchanger was inhibited by application of 20 µM CGP37157 (Suppl. Fig. 3B,D), but this had neither a significant effect on the number of 'active' microglia (47.7 ± 4.0%, n = 31/985, $p = 0.6913$ compared to control) nor on the frequency of the events (5.0 ± 0.5 events/hour and cell, $p = 0.2091$ compared to control). Taken together, these data indicate that spontaneous Ca^{2+} transients in cultured microglia emerge mainly from Ca^{2+} release from internal ER stores.

3.3. Endoplasmic reticulum (ER) Ca^{2+} channels contribute to spontaneous transients in microglia

Two families of Ca^{2+}-permeable ion channels are presently known to be expressed in ER membranes, namely the inositol-1, 4, 5-trisphosphate receptors (IP_3R) and the ryanodine receptors (RyR). We tested if spontaneous Ca^{2+} transients in cultured microglia depend on the activity of these channels. In order to identify the contribution of RyR and IP_3R on the spontaneous Ca^{2+} transients, IP_3R activity was inhibited by U73122 (20 µM), and RyR activity by ryanodine (20 µM). Blockade of IP_3Rs by washing in U73122, an inhibitor of PLC, abolished spontaneous Ca^{2+} transients completely (0.2± 0.0 events per hour and cell, n = 797 cells, 10 coverslips 4 culture preparations, $p < 0.0001$ compared to control). As shown in Fig. 3C,D and E, ryanodine had no effect on the occurrence of spontaneous Ca^{2+} transients. In the presence of ryanodine, 33.2 ± 2.4% of the microglia displayed spontaneous activity (n = 889 cells, 11 coverslips, 3 culture preparations, $p = 0.9880$ compared to control), and the frequency was 3.35 ± 0.21 events per hour and cell ($p = 0.0701$). We also investigated the effect of 10 mM caffeine,

which activates RyR and antagonizes IP_3R [24-27] and should therefore block phasic activity of both receptor families in cultured neonatal microglia. Application of 10 mM caffeine (n = 751 cells, 12 coverslips, 4 culture preparations) led indeed to a complete loss of spontaneous Ca^{2+} transients in neonatal cultured microglia (Fig. 3A and E), further supporting an ER release mechanism.

The main contribution of IP_3R to the spontaneous Ca^{2+} transients is also in line with data on the mRNA expression of IP_3R1-3 and RyR1-3 in our neonatal microglia cultures. As shown in figure 3B, all IP_3R isoforms were expressed at high levels whereas RyR1 and RyR3 transcripts could be detected only at sparse expression levels in our neonatal microglia preparation. In summary, we conclude that spontaneous Ca^{2+} transients in microglia are dependent on endoplasmic Ca^{2+} channels which are predominantly formed by IP_3R subunits.

3.4. Auto-/ paracrine purinergic signaling is not the trigger for spontaneous intracellular Ca^{2+} elevations in microglia.

Many isoforms of purinergic P2Y receptors are expressed on microglia, and their downstream signaling includes the activation of PLC and Ca^{2+} elevation from internal stores [5, 12]. We therefore asked if spontaneous Ca^{2+} transients in microglia might be triggered by autocrine ATP release and subsequent activation of P2Y receptors. In a first set of experiments, we tested if the manipulation of putatively released ATP has an influence on the occurrence of spontaneous Ca^{2+} transients. Apyrase (10 U/ml), an enzyme catalyzing the degradation of ATP to ADP and AMP, was applied during Ca^{2+} imaging experiments. As shown in the left panel of Fig.4A, this failed to block spontaneous Ca^{2+} transients, and the frequency (26.5 ± 5.6. n = 257 cells, 14 coverslips, 3 culture preparations; $p = 0.0168$) was even increased compared to control conditions, arguing against an ATP-dependent triggering mechanism. We also tested microglia derived from $CD39^{-/-}$ animals which lack the intrinsic apyrase activity of the transmembrane protein CD39 and should therefore display higher extracellular ATP levels if substantial release occurred. However, there was no change in the frequency of spontaneous Ca^{2+} transients in neonatal $CD39^{-/-}$ cultured microglia (11.6 ± 1.0; n = 1587 cells, 33 coverslips, 4 culture preparations; $p = 0.6600$; Fig. 4A *middle* and *right*). These data do support an ATP-independent trigger of spontaneous Ca^{2+} transients. To further confirm this notion, we next investigated possible phasic ATP release pathways. Exocytosis of ATP-containing vesicles is one of these, and was previously shown to be sensitive to treatment of Bafilomycin in neonatal cultured microglia from rat [28]. Bafilomycin is an inhibitor of vesicular H^+ transporters, perishing the lysosomal H^+ gradient and therefore abolishing ATP loading of the vesicles. We incubated

microglia for 12 h with 500 nM Bafilomycin and compared spontaneous Ca^{2+} elevations with control microglia that were incubated for the same period without any agent. However, no changes were observed in the frequency (5.8 ± 1.1 events/cell*h; n = 728 cells, 9 coverslips, 4 culture preparations; p = 0.1645; Fig. 4B *left* and *right*) or kinetics of the events (11.8 ± 1.0 s, p = 0.5540 and 14.4 ± 0.7 s, p = 0.2416 for rise and decay times, respectively, data not shown). Phasic ATP release might also occur through large pore ion channels, including connexin hemichannels or $P2X_7$ receptors [29]. As shown in Fig. 4B *middle*, blocking connexin hemichannel conductance using 50 µM carbenoxolone did not alter the frequency significantly (4.6 ± 0.6 events/cell*h, p = 0.1009, n = 898 cells, 11 coverslips, 3 culture preparations), but the application of 100 µM PPADS to inhibit P2X receptors led to a dramatic increase in the frequency of spontaneous Ca^{2+} transients (25.3 ± 3.7 events/cell*h p = 0.0007, n = 464 cells, 11 coverslips, 1 culture preparation; Fig. 4C, *middle*). Interestingly, by the application of each of the two channel inhibitors, there was a significant decrease in rise times (8.2 ± 0.5 s, $p < 0.001$ and 7.6 ± 0.4 s, $p < 0.001$ for carbenoxolone and PPADS, respectively) and in decay times (10.0 ± 0.5 s, $p < 0.001$ and 8.8 ± 0.6 s, $p < 0.001$ for carbenoxolone and PPADS, respectively) of the spontaneous Ca^{2+} transients. In summary, we conclude that the ion channel conductance through connexin hemichannels and P2X receptors contributes to the modulation of spontaneous Ca^{2+} transients in microglia but does not trigger their occurrence. We finally investigated if block of P2Y receptors impedes spontaneous Ca^{2+} transients in microglia. The application of reactive blue (RB2) increased the frequency of Ca^{2+} transients instead of blocking them (n = 302 cell, 19 coverslips, 2 culture preparations. As shown in Fig. 4C *right*, the events occurred at such a high frequency that analysis of their kinetics of frequency was not possible. Since RB2 is a rather unspecific drug acting on several other cellular components including P2X receptors, we also blocked P2Y receptor isoforms more specifically using suramin (inhibitor for $P2Y_{2,4,12}$ but also for P2X receptors, n = 892 cells, 13 coverslips, 4 culture preparations) and MRS2573 (inhibitor for $P2Y_6$ n = 721 cells, 11 coverslips, 3 culture preparations). However, as shown in Fig. 4D, spontaneous Ca^{2+} transients did not change significantly under these treatments. Taken together, we conclude that autocrine purinergic signaling is unlikely to be the trigger of spontaneous Ca2+ transients in microglia.

3.5. Spontaneous Ca^{2+} transients are differentially shaped under patho-physiological conditions.

We finally tested if spontaneous Ca^{2+} transients are associated with patho-physiological functions of microglia. Lipopolysaccharide (LPS) is the major component of the outer membrane of Gram-negative bacteria and activates TLR4 receptors in microglia resulting in an

inflammatory response characterized by release of cytokines and NO [30]. We used 100 ng/ml LPS in acute and two chronic experimental paradigms. As shown in Fig. 5B, application of LPS during the recording did not significantly increase the frequency of spontaneous Ca^{2+} transients in neonatal cultured microglia compared to control conditions (7.0 ± 1.5 events per hour and cell, n = 799 cells, 13 coverslips, 3 culture preparations, p = 0.6587), and also the rise (11.4 ± 0.5 s; p = 0.0705) and decay times (12.5 ± 0.6 s; p = 0.1421) were largely unaffected. In contrast, chronic treatment of cultured microglia for 12h significantly prolonged the kinetics of spontaneous Ca^{2+} transients (Fig. 5C,F), resulting in longer rise times of 16.6 ± 1.1 s (n = 516 cells. 9 coverslips, 3 culture preparations, p < 0.001) and decay times of 18.8 ± 1.2 s (p < 0.0001). The kinetics after LPS treatment of microglia for 36h were also slower, being 17.8 ± 0.8 s (rise time, n =472 cells, coverslips, 3 culture preparations 9/472, p < 0.0001 compared to control) and 22.1 ± 1.4 s (decay time, p < 0.0001 compared to control) but the frequency of spontaneous Ca^{2+} transients recovered compared to 12 h LPS treatment, and was not significantly different any more from control conditions (2.4 ± 0.3 events/cell*h, p = 0.0854; Fig. 5E). In summary, the appearance and occurrence of spontaneous Ca^{2+} transients in microglia changes time-dependently during chronic LPS treatment whereas acute LPS administration has no influence.

We investigated glioma-associated microglia isolated from GL261-derived tumors (mGAM: mouse glioma-associated microglia; see materials and methods and Suppl. Fig. 2). Compared to freshly-isolated microglia, spontaneous Ca^{2+} transients from mGAM's (Fig. 6A) appeared at similar frequencies (2.2 ± 0.3 events per hour and cell, n = 423 cells, 9 coverslips, 3 animals, p = 0.5558; Fig. 6C), but their rise and decay kinetics were significantly faster (11.1 ± 1.6 s and 18.4 ± 0.8 s, p = 0.0468 and p = 0.0017 for rise and decay times, respectively, Fig. 6D). Thus, the tumor context alters the kinetics of spontaneous Ca^{2+} transients in microglia, but different from chronic LPS treatment. We finally also characterized human brain macrophages/microglia derived from surgery tumor resections (hGAM's; Fig. 6B and Suppl. Fig. 2). Like mouse microglia, hGAM's displayed spontaneous Ca^{2+} transients at frequencies comparable with freshly-isolated mouse microglia (2.4 ± 0.3 events per hour and cell, n = 641 cells, 8 coverslips, 3 tumors, p = 0.3318; Fig. 6B, C). These data show that the appearance of spontaneous Ca^{2+} transients is not specific to mouse but also occurs in human brain macrophages/microglia.

4. Discussion

Cytosolic Ca^{2+} elevations are important intracellular signals involved in many cellular processes like cell proliferation, apoptosis, gene expression and also in more specific cellular functions like muscle contraction or synaptic transmission [15]. It is known and accepted for a long time that microglia respond to various physiological and patho-physiological stimuli with elevations in their intracellular Ca^{2+} levels. In the present study, we describe spontaneous, transient Ca^{2+} elevations in microglia isolated and purified from brain tissue. Similarly, we recorded these events in purified microglial cultures, and these events were not dependent on the cell density of the cultures. Previous studies conducted *in vivo* on microglia also reported spontaneous Ca^{2+} transients [18, 19], but were actually not suitable to distinguish between external, non-microglial and intrinsic microglial triggering of these events. In the present study we could show these responses in different isolated microglial preparations, under physiological and pathophysiological conditions, therefore suggesting that this type of activity represents an intrinsic property of microglia.

Spontaneous Ca^{2+} transients were shown in the present study to be generated by Ca^{2+} release from internal stores. We have found that store depletion (CPA, thapsigargin), PLC inhibition (U73122) as well as blockade of IP_3Rs abolished spontaneous Ca^{2+} transients, indicating that the transients are due to release from cytoplasmic stores rather than Ca^{2+} entry from extracellular space. Spontaneous cytosolic Ca^{2+} elevations arising from the ER were previously described in many excitable and non-excitable isolated cell types, including neutrophils [31], myocytes [32, 33], interstitial cells [34], astrocytes [35] and neurons [36]. However, in many of these cell preparations, spontaneous cytosolic calcium elevations occur at much higher frequencies, being rather oscillatory than stochastically distributed. Consistently, RyRs and calcium-induced calcium release [37] were shown to be responsible for the occurrence of cytosolic Ca^{2+} transients. In microglia, we have shown that spontaneous cytosolic Ca^{2+} transients are due to the phasic activity of IP_3Rs, raising the question for the superordinate signaling that triggers those events. Microglial cells express a plethora of G_qPCR receptors which could trigger IP_3R-mediated Ca^{2+} release [5], including purinoreceptors. However, neuron- or macroglia-provided extracellular ligands are absent since our cultures or the freshly isolated population contained microglia only. Thus, as a possible mechanism, an autocrine release and signaling mechanism could be considered such as ATP release and activation of purinergic signaling. The functional expression of several P2Y receptor isoforms is a well-known characteristic of microglia *in vitro [38-40]* and *in situ [41, 42]*, and intracellular Ca^{2+} elevations mediated by these receptors can be triggered directly by application of purines or by purine

release through tissue damage. Intriguingly, many of the P2Y receptors expressed in microglia are coupled to $G\alpha_q$, and thus to IP_3R-dependent intracellular Ca^{2+} elevations. Phasic purine release from microglia was indeed previously shown to occur through bafilomycin-sensitive, vesicular release [28] and also via non-lytic mechanisms [43, 44]. However, in the current study, inhibition of these possible ATP release pathways did not lead to a loss of spontaneous Ca^{2+} transients. Conversely, their frequency was drastically increased when either 50 µM RB2, 100 µM PPADS or 10 U/ml apyrase were applied. The reason for this upregulation might be explained by the fact that these substances interact with several P2X/Y receptors at the same time, and that the cumulative action leads to an increase in frequency. However, since all of these substances are relatively unspecific and prone to interact with many off-target molecules, the reason for the frequency increases after RB2-, PPADS-, or apyrase treatment remains elusive. However, we can conclude from our data that it is very unlikely that P2XR's and /or P2YR's trigger spontaneous Ca^{2+} transients in microglia because blocking them should in that case inevitably lead to a complete loss of the spontaneous Ca^{2+} transients, which was not the case. A further indication against a paracrine purinergic signaling loop is the observation that the events occurred independently of the density of microglial cultures. The mechanism which triggers the spontaneous Ca^{2+} transients in microglia remains thus elusive.

Previous studies described spontaneous Ca^{2+} transients in microglia *in vivo* [18, 19], and these events are similar as the ones described in our study. First, the percentages of 'active' microglia, i.e. those cells that display at least one transient during the recording period, were similar. Eichhoff *et al.* [18] found that around 22% of the microglia of 2-4 months old $CX_3CR1^{+/GFP}$ mice were spontaneously active, whereas we found transients in 25.2 ± 4.1% of adult (P60-P70) microglia. Second, rise and decay kinetics of microglial Ca^{2+} transients *in vitro* and *in vivo* resemble each other and are in the range of 10-13 s [18]. Similarities are, third, also abundant pharmacologically: Like in the living animal [19], spontaneously occurring Ca^{2+} elevations of isolated microglia could be abolished by application of CPA in our preparations and are therefore consistently dependent on release mechanisms from intracellular Ca^{2+} stores. Furthermore, Eichhoff *et al.*, showed *in vivo* that spontaneous Ca^{2+} transients in microglia do not depend on astrocytic Ca^{2+} waves or neuronal activity, which is in line with our finding that spontaneous Ca^{2+} transients do also occur in isolated microglia preparations, and which contradicts the hypothesis of Verderio and Matteoli [17] that astrocytic ATP release is the major determinant of spontaneous Ca^{2+} transients in microglia. However, Eichhoff *et al. [18] and* Brawek *et al. [19]* propose a tissue-dependent mechanism that includes "minor cell/tissue damages in the vicinity of microglial cells" as a local source of ATP that activates microglial P2Y

receptors. Although we explicitly do not rule out that this might take place under physiological or pathophysiological conditions in the living brain, we suggest that there must be a further abundant autocrine mechanism evoking spontaneous Ca^{2+} transients in microglia (see above).

Microglia *in vivo* display a different - more ramified - morphology than freshly-isolated or cultured microglia (see Suppl. Fig. 2B). This morphological change is associated with a stage of microglial activation states which may differ with different isolation procedures. This activation state can affect intracellular functions and pathways such as the resting Ca^{2+} concentration which is elevated when microglia are stimulated with LPS [30]. However, the general ability of microglia to produce spontaneous Ca^{2+} transients indicates that the molecular mechanism which generates these events was present in all the different microglial preparations.

In the present study, we also investigated spontaneous Ca^{2+} transients occurring under pathophysiological conditions. We observed these responses after prolonged treatment with LPS and in glioma-associated microglia. We found minor changes in the frequency of events but pronounced effects on their kinetics, indicating alterations in the functional expression or in the activity of proteins that are involved in intracellular Ca^{2+} homeostasis. LPS stimulation was shown to elevate the resting level of cytoplasmic Ca^{2+} concentration and to modulate purinergic signaling [10, 30]. Our data extend this finding to spontaneous Ca^{2+} transients which are less frequent and have slower rise and decay kinetics after 12h treatment with LPS. Interestingly, in plaque-associated microglia from mouse models of Alzheimer's disease, spontaneous Ca^{2+} transients were previously shown to occur much more frequently [19]. Additionally, the kinetics and extend of events (measured there as area under the curve) were also changed under disease conditions. This further emphasizes our conclusion that spontaneous Ca^{2+} transients in microglia reflect aspects of their cellular homeostasis and activation state. Future studies will have to show if and to which extend these phasic Ca^{2+} elevations contribute to the physiological and patho-physiological features of microglia.

Acknowledgements

We thank Regina Piske, Maren Wendt, Hanna Schmidt and Irene Haupt for excellent technical assistance. This work was supported by Deutsche Forschungsgemeinschaft (SFB TRR 43), Neurocure and the DAAD.

References

[1] A. Nimmerjahn, F. Kirchhoff, F. Helmchen, Resting microglial cells are highly dynamic surveillants of brain parenchyma in vivo, Science (New York, N.Y.), 308 (2005) 1314-1318.
[2] S. Koizumi, Y. Shigemoto-Mogami, K. Nasu-Tada, Y. Shinozaki, K. Ohsawa, M. Tsuda, B.V. Joshi, K.A. Jacobson, S. Kohsaka, K. Inoue, UDP acting at P2Y6 receptors is a mediator of microglial phagocytosis, Nature, 446 (2007) 1091-1095.
[3] D. Davalos, J. Grutzendler, G. Yang, J.V. Kim, Y. Zuo, S. Jung, D.R. Littman, M.L. Dustin, W.B. Gan, ATP mediates rapid microglial response to local brain injury in vivo, Nature neuroscience, 8 (2005) 752-758.
[4] U.K. Hanisch, H. Kettenmann, Microglia: active sensor and versatile effector cells in the normal and pathologic brain, Nature neuroscience, 10 (2007) 1387-1394.
[5] H. Kettenmann, U.K. Hanisch, M. Noda, A. Verkhratsky, Physiology of microglia, Physiological reviews, 91 (2011) 461-553.
[6] S.E. Haynes, G. Hollopeter, G. Yang, D. Kurpius, M.E. Dailey, W.B. Gan, D. Julius, The P2Y12 receptor regulates microglial activation by extracellular nucleotides, Nature neuroscience, 9 (2006) 1512-1519.
[7] K. Ohsawa, Y. Irino, Y. Nakamura, C. Akazawa, K. Inoue, S. Kohsaka, Involvement of P2X4 and P2Y12 receptors in ATP-induced microglial chemotaxis, Glia, 55 (2007) 604-616.
[8] M.A. Petersen, M.E. Dailey, Diverse microglial motility behaviors during clearance of dead cells in hippocampal slices, Glia, 46 (2004) 195-206.
[9] A. Rappert, I. Bechmann, T. Pivneva, J. Mahlo, K. Biber, C. Nolte, A.D. Kovac, C. Gerard, H.W. Boddeke, R. Nitsch, H. Kettenmann, CXCR3-dependent microglial recruitment is essential for dendrite loss after brain lesion, The Journal of neuroscience : the official journal of the Society for Neuroscience, 24 (2004) 8500-8509.
[10] T. Moller, O. Kann, A. Verkhratsky, H. Kettenmann, Activation of mouse microglial cells affects P2 receptor signaling, Brain research, 853 (2000) 49-59.
[11] T. Moller, J.J. Contos, D.B. Musante, J. Chun, B.R. Ransom, Expression and function of lysophosphatidic acid receptors in cultured rodent microglial cells, The Journal of biological chemistry, 276 (2001) 25946-25952.
[12] K. Farber, H. Kettenmann, Functional role of calcium signals for microglial function, Glia, 54 (2006) 656-665.
[13] D.K. Heo, H.M. Lim, J.H. Nam, M.G. Lee, J.Y. Kim, Regulation of phagocytosis and cytokine secretion by store-operated calcium entry in primary isolated murine microglia, Cellular signalling, 27 (2015) 177-186.
[14] M. Michaelis, B. Nieswandt, D. Stegner, J. Eilers, R. Kraft, STIM1, STIM2, and Orai1 regulate store-operated calcium entry and purinergic activation of microglia, Glia, 63 (2015) 652-663.
[15] D.E. Clapham, Calcium Signaling, Cell, 131 (2007) 1047-1058.
[16] C.C. Hegg, S. Hu, P.K. Peterson, S.A. Thayer, Beta-chemokines and human immunodeficiency virus type-1 proteins evoke intracellular calcium increases in human microglia, Neuroscience, 98 (2000) 191-199.
[17] C. Verderio, M. Matteoli, ATP Mediates Calcium Signaling Between Astrocytes and Microglial Cells: Modulation by IFN- The Journal of Immunology, 166 (2001) 6383-6391.
[18] G. Eichhoff, B. Brawek, O. Garaschuk, Microglial calcium signal acts as a rapid sensor of single neuron damage in vivo, Biochimica et biophysica acta, 1813 (2011) 1014-1024.
[19] B. Brawek, B. Schwendele, K. Riester, S. Kohsaka, C. Lerdkrai, Y. Liang, O. Garaschuk, Impairment of in vivo calcium signaling in amyloid plaque-associated microglia, Acta neuropathologica, 127 (2014) 495-505.

[20] M. Nikodemova, J.J. Watters, Efficient isolation of live microglia with preserved phenotypes from adult mouse brain, Journal of neuroinflammation, 9 (2012) 147.
[21] M. Olah, D. Raj, N. Brouwer, A.H. De Haas, B.J. Eggen, W.F. Den Dunnen, K.P. Biber, H.W. Boddeke, An optimized protocol for the acute isolation of human microglia from autopsy brain samples, Glia, 60 (2012) 96-111.
[22] J. Ye, G. Coulouris, I. Zaretskaya, I. Cutcutache, S. Rozen, T.L. Madden, Primer-BLAST: a tool to design target-specific primers for polymerase chain reaction, BMC bioinformatics, 13 (2012) 134.
[23] B.S. Khakh, G. Burnstock, C. Kennedy, B.F. King, R.A. North, P. Seguela, M. Voigt, P.P. Humphrey, International union of pharmacology. XXIV. Current status of the nomenclature and properties of P2X receptors and their subunits, Pharmacological reviews, 53 (2001) 107-118.
[24] T. Ozawa, Modulation of ryanodine receptor Ca2+ channels (Review), Molecular medicine reports, 3 (2010) 199-204.
[25] I. Bezprozvanny, S. Bezprozvannaya, B.E. Ehrlich, Caffeine-induced Inhibition of Inositol(1,4,5)-

Trisphosphate-gated Calcium Channels

from Cerebellum, Molecular Biology of the Cell, 5 (1990) 97-103.
[26] H. Saleem, S.C. Tovey, T.F. Molinski, C.W. Taylor, Interactions of antagonists with subtypes of inositol 1,4,5-trisphosphate (IP3) receptor, British journal of pharmacology, 171 (2014) 3298-3312.
[27] W. Huang, M.C. Cane, R. Mukherjee, P. Szatmary, X. Zhang, V. Elliott, Y. Ouyang, M. Chvanov, D. Latawiec, L. Wen, D.M. Booth, A.C. Haynes, O.H. Petersen, A.V. Tepikin, D.N. Criddle, R. Sutton, Caffeine protects against experimental acute pancreatitis by inhibition of inositol 1,4,5-trisphosphate receptor-mediated Ca2+ release, Gut, (2015).
[28] Y. Dou, H.J. Wu, H.Q. Li, S. Qin, Y.E. Wang, J. Li, H.F. Lou, Z. Chen, X.M. Li, Q.M. Luo, S. Duan, Microglial migration mediated by ATP-induced ATP release from lysosomes, Cell research, 22 (2012) 1022-1033.
[29] A.W. Lohman, M. Billaud, B.E. Isakson, Mechanisms of ATP release and signalling in the blood vessel wall, Cardiovascular research, 95 (2012) 269-280.
[30] A. Hoffmann, O. Kann, C. Ohlemeyer, U.K. Hanisch, H. Kettenmann, Elevation of basal intracellular calcium as a central element in the activation of brain macrophages (microglia): suppression of receptor-evoked calcium signaling and control of release function, The Journal of neuroscience : the official journal of the Society for Neuroscience, 23 (2003) 4410-4419.
[31] M.E. Jaconi, R.W. Rivest, W. Schlegel, C.B. Wollheim, D. Pittet, P.D. Lew, Spontaneous and chemoattractant-induced oscillations of cytosolic free calcium in single adherent human neutrophils, The Journal of biological chemistry, 263 (1988) 10557-10560.
[32] D.A. Williams, L.M. Delbridge, S.H. Cody, P.J. Harris, T.O. Morgan, Spontaneous and propagated calcium release in isolated cardiac myocytes viewed by confocal microscopy, The American journal of physiology, 262 (1992) C731-742.
[33] H. Satoh, L.A. Blatter, D.M. Bers, Effects of [Ca2+]i, SR Ca2+ load, and rest on Ca2+ spark frequency in ventricular myocytes, The American journal of physiology, 272 (1997) H657-668.
[34] L. Johnston, G.P. Sergeant, M.A. Hollywood, K.D. Thornbury, N.G. McHale, Calcium oscillations in interstitial cells of the rabbit urethra, The Journal of physiology, 565 (2005) 449-461.
[35] T.F. Wang, C. Zhou, A.H. Tang, S.Q. Wang, Z. Chai, Cellular mechanism for spontaneous calcium oscillations in astrocytes, Acta pharmacologica Sinica, 27 (2006) 861-868.
[36] A. Verkhratsky, A. Shmigol, Calcium-induced calcium release in neurones, Cell calcium, 19 (1996) 1-14.
[37] M. Endo, Calcium-induced calcium release in skeletal muscle, Physiological reviews, 89 (2009) 1153-1176.

[38] J.G. McLarnon, Purinergic mediated changes in Ca2+ mobilization and functional responses in microglia: effects of low levels of ATP, Journal of neuroscience research, 81 (2005) 349-356.
[39] A.R. Light, Y. Wu, R.W. Hughen, P.B. Guthrie, Purinergic receptors activating rapid intracellular Ca increases in microglia, Neuron glia biology, 2 (2006) 125-138.
[40] S. Visentin, C.D. Nuccio, G.C. Bellenchi, Different patterns of Ca(2)(+) signals are induced by low compared to high concentrations of P2Y agonists in microglia, Purinergic signalling, 2 (2006) 605-617.
[41] Y. Sasaki, M. Hoshi, C. Akazawa, Y. Nakamura, H. Tsuzuki, K. Inoue, S. Kohsaka, Selective expression of Gi/o-coupled ATP receptor P2Y12 in microglia in rat brain, Glia, 44 (2003) 242-250.
[42] C. Boucsein, R. Zacharias, K. Farber, S. Pavlovic, U.K. Hanisch, H. Kettenmann, Purinergic receptors on microglial cells: functional expression in acute brain slices and modulation of microglial activation in vitro, The European journal of neuroscience, 17 (2003) 2267-2276.
[43] D. Ferrari, P. Chiozzi, S. Falzoni, M. Dal Susino, G. Collo, G. Buell, F. Di Virgilio, ATP-mediated cytotoxicity in microglial cells, Neuropharmacology, 36 (1997) 1295-1301.
[44] A. Cisneros-Mejorado, A. Perez-Samartin, M. Gottlieb, C. Matute, ATP signaling in brain: release, excitotoxicity and potential therapeutic targets, Cellular and molecular neurobiology, 35 (2015) 1-6.

Figures

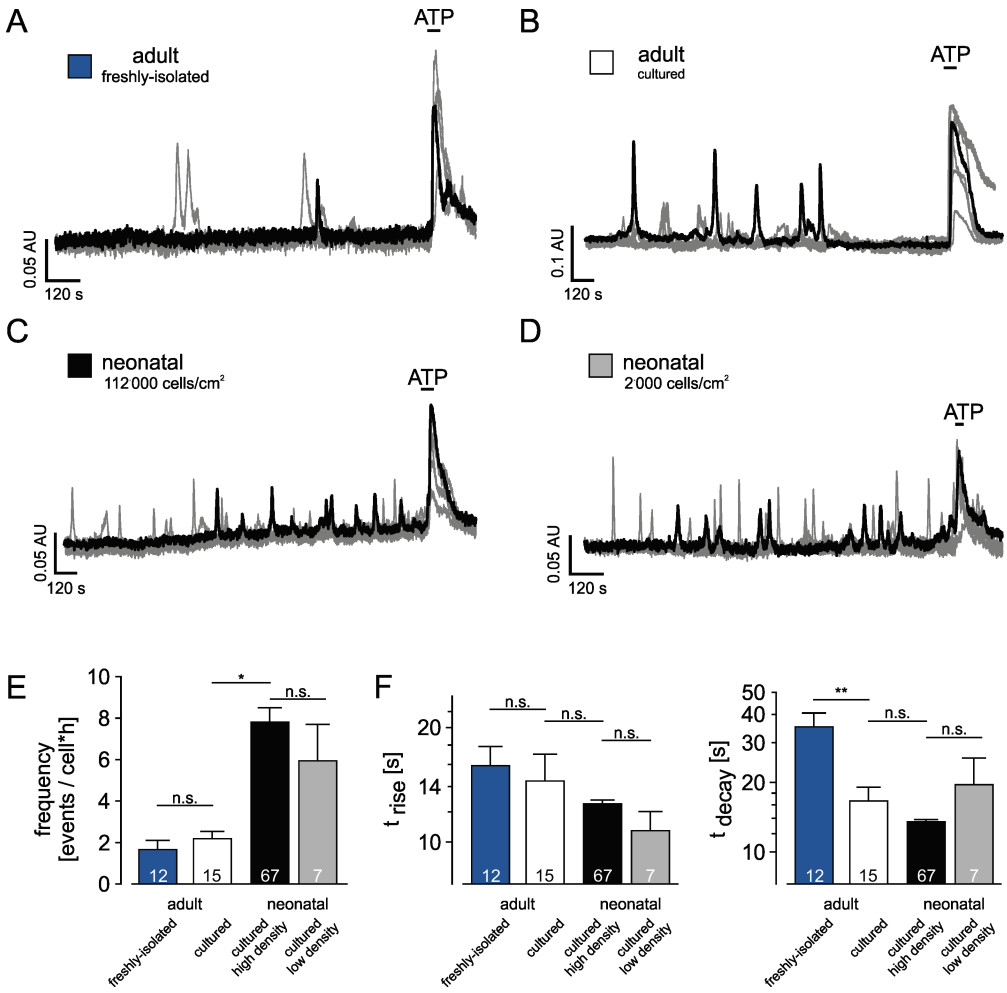

Figure 1. Spontaneous cytosolic Ca^{2+} transients in microglia.

A - D. Sample traces of Ca^{2+} recordings from freshly-isolated adult microglia (P50-P70, A), from adult cultured microglia (P50-P70;B) or from neonatal (P0-P3) cultured microglia seeded at 150000 microglia per coverslip (C) or 2500 microglia per coverslip (D). Cells were loaded with the membrane-permeable Ca^{2+} indicator Fluo4®-AM to measure changes in cytosolic Ca^{2+} (for a sample image see Suppl. Fig. 1D). The traces show representative traces from 5 regions of interest on one coverslip. Note that for each microglia preparation, a similar subset of microglia displayed spontaneous cytosolic Ca^{2+} transients, i.e. without application of any substance. At the end of each experiment, 1 mM ATP was applied as a control in these and all subsequent experiments. **E.** The mean frequency of spontaneous Ca^{2+} transients for freshly-isolated adult microglia (blue bar), adult cultured microglia (white bar), neonatal cultured microglia seeded at 150000 microglia per coverslip (black bar) or 2500 microglia per coverslip (white bar). **F.** Summary of rise (left) and decay (right) times of Ca^{2+} transients for the four microglial preparations. Color code of the bars is as in E. Please note that data rise and decay times are plotted logarithmically. Statistics: n.s.: not significant; **p<0.01. Numbers on the bars indicate the number of experiments (coverslips).

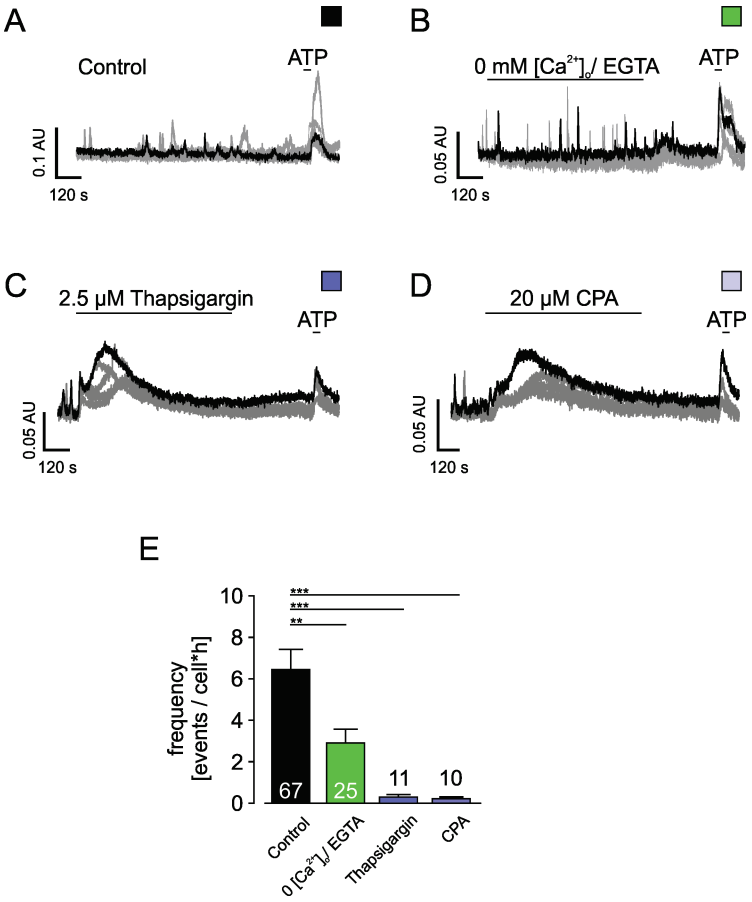

Figure 2 Spontaneous Ca^{2+} transients in microglia arise from the ER.

A. Representative traces of an experiment on neonatal cultured microglia under control conditions. Cytosolic Ca^{2+} was imaged for 15 min in standard extracellular solution, and 1 mM ATP was applied as a control at the end of each recording. **B.** During the removal of extracellular Ca^{2+}(as indicated by bar), spontaneous microglial Ca^{2+} transients were still present. **C and D.** Depletion of the internal ER Ca^{2+} stores due to the blockade of SERCA by 20 µM thapsigargin (C) or 20 µM CPA (D) abolished spontaneous Ca^{2+} transients in microglia. **E.** Summary of the frequency of microglial spontaneous Ca^{2+} transients under control (black) and Ca^{2+}-free conditions (green) and after store depletion (purple = CPA; light purple = thapsigargin). Statistics: n.s.: not significant **: $p<0.01$; ***: $p<0.001$. Numbers on the bars indicate the number of experiments (coverslips).

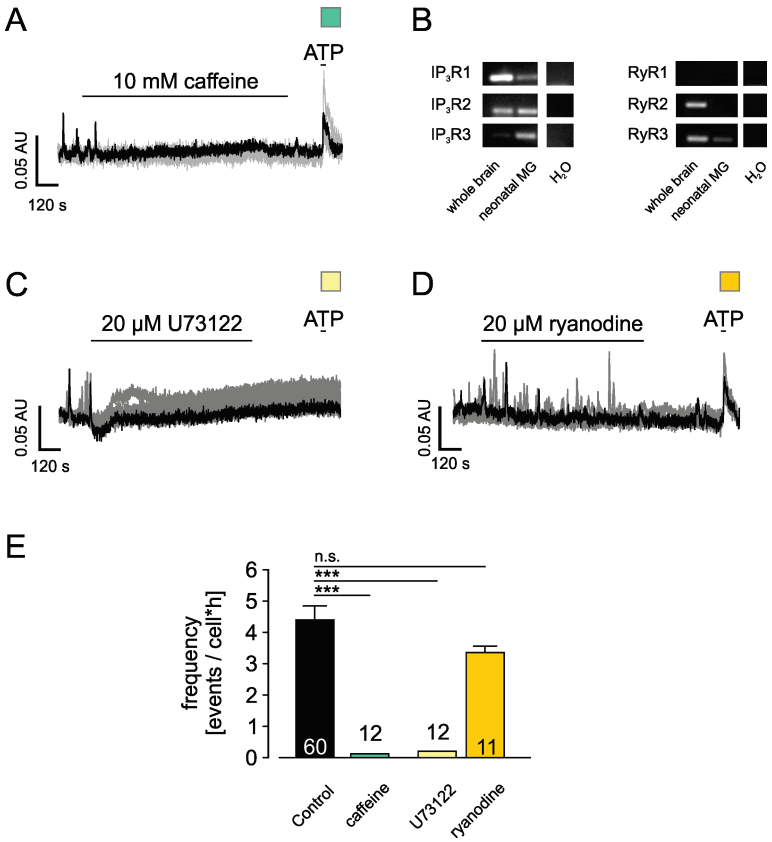

Figure 3 ER Ca^{2+} channels contribute to spontaneous Ca^{2+} transients in microglia.

A. Caffeine completely blocked spontaneous Ca^{2+} transients in neonatal microglia cultures. **B.** mRNA expression of IP_3R (left) and RyR isoforms (right) in neonatal cultured microglial cells compared to whole brain and an H_2O control. **C.** Inhibition of IP_3R by PLC blockade (20 µM U73122,) abolished spontaneous Ca^{2+} transients in microglia. **D.** RyR inhibition by ryanodine (20 µM) had no effect on spontaneous Ca^{2+} transients in microglia. **E.** Summary of the frequency of microglial spontaneous Ca^{2+} transients under control conditions (black) and in the presence of 10 mM caffeine (blue), 20 µM U73122 (beige) or 20 µM ryanodine (yellow). Statistics: n.s.: not significant ***: $p<0.001$;. Numbers on the bars indicate the number of experiments (coverslips). Substance applications are indicated by bar.

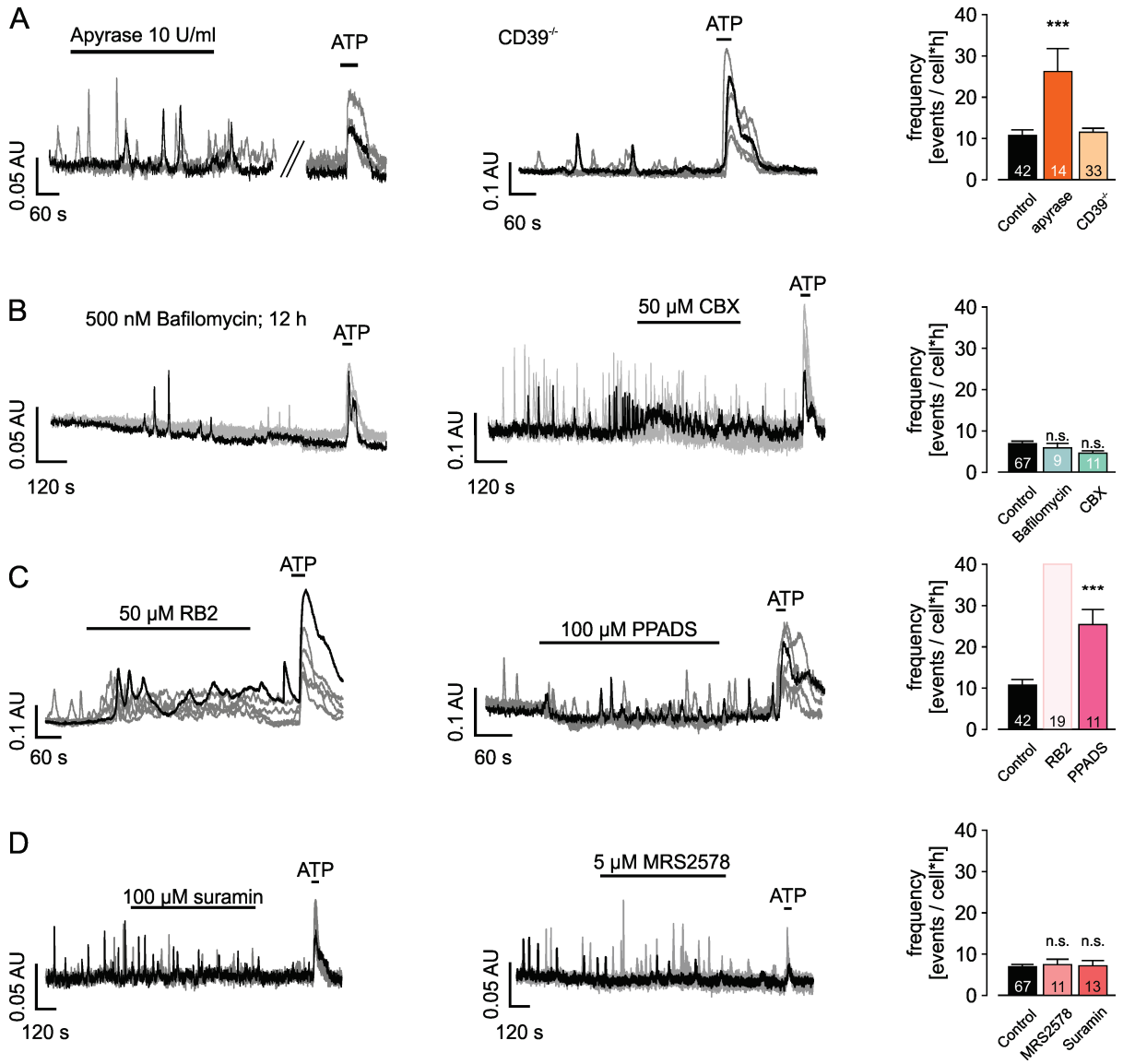

Figure 4. Mediators of autocrine purinergic signalling do not block spontaneous Ca^{2+} transients.

A. *left,* Representative traces from an experiment on neonatal cultured microglia during applicationof 10 U/ml apyrase. *middle*, Neonatal cultured microglia from CD39$^{-/-}$ animals display spontaneous Ca^{2+} transients similar to wild type microglia. *Right,* Summary of the frequencies of microglial spontaneous Ca^{2+} transients under control conditions (black), during application of apyrase (orange) of in CD39$^{-/-}$ microglia. **B.** Sample traces from neonatal cultured microglia treated for 12 h with Bafilomycin (*top*) or treated acutely with 50 µM carbenoxolone (CBX, *middle*). The frequencies (*right*) were not different from microglia under control conditions. **C.** Inhibition of purinergic receptors with 50 µM reactive blue (RB2, *left*) or 100 µM PPADS (*middle*) led to significant increases in the frequency of spontaneous Ca^{2+} transients (*right*). PLease note that in the case of RB2, it was not possible to reliably analyse single transients. **D.** 100 µM suramin ($P2Y_{2,4,12}$, *left*) or 5 µM MRS2578 ($P2Y_6$, *middle*) had no influence on the occurrence of spontaneous Ca^{2+} transients in neonatal cultured microglia. Summary is shown in the *right* panel. Statistics: n.s.: not significant; ***: p<0.001. Numbers on the bars indicate the number of experiments (coverslips).

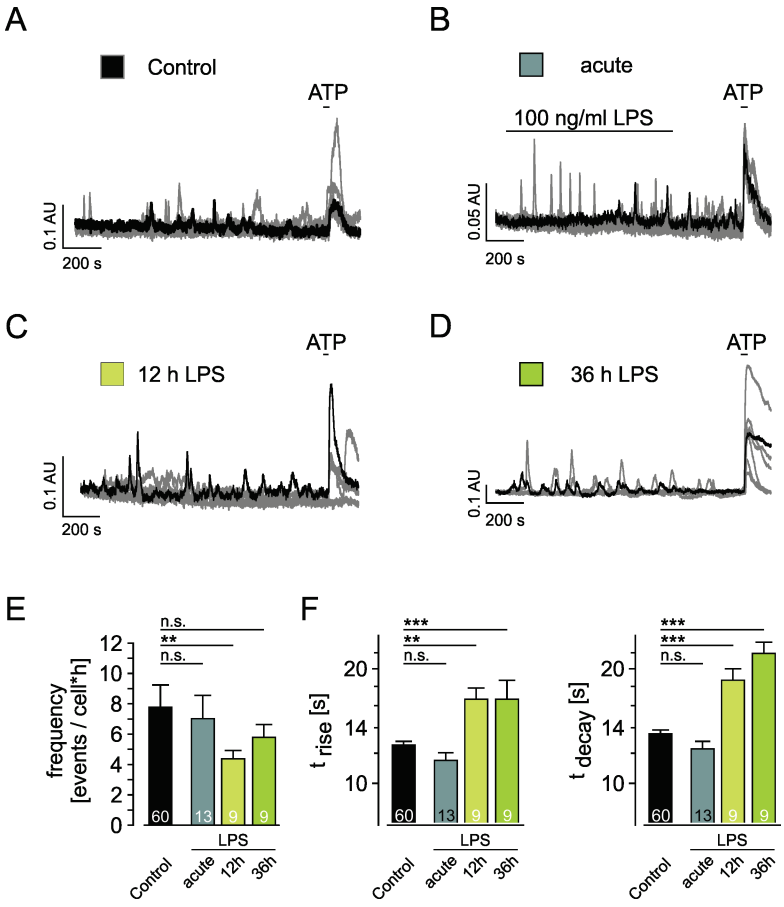

Figure 5. LPS modulates spontaneous Ca^{2+} transients in microglia.

A-D. Representative traces of experiments on untreated (A) neonatal cultured microglia under control conditions. In the experiment shown B, 100 ng/ml LPS was applied for 15 min during the recording as indicated by bar. Ca^{2+} recordings in C and D are from microglia after treatment with 100 ng/ml LPS for 12 h (C) or 36 h (D) prior to Ca^{2+} imaging. Statistics: n.s., not significant; *, $p < 0.05$; *, $p < 0.05$; *, $p < 0.05$. **E.** Mean frequency of microglial spontaneous Ca^{2+} transients under control conditions (black), with acute LPS stimulation during the recording (gray) or with microglia treated for 12 h (light green) or 36 h (green) with LPS. Statistics: **p<0.01; n.s., not significant. Numbers on the bars indicate the number of experiments (coverslips). **F.** Summary of the rise (left) and decay (right) times of spontaneous Ca^{2+} transients in neonatal microglia under control conditions, with acute LPS stimulation during the recording or with microglia treated for 12 h or 36 h with LPS. Colour code is as in E. Note that data rise and decay times are plotted logarithmically. Statistics: n.s.: not significant; **: p<0.01; ***: p<0.001. Numbers on the bars indicate the number of experiments (coverslips).

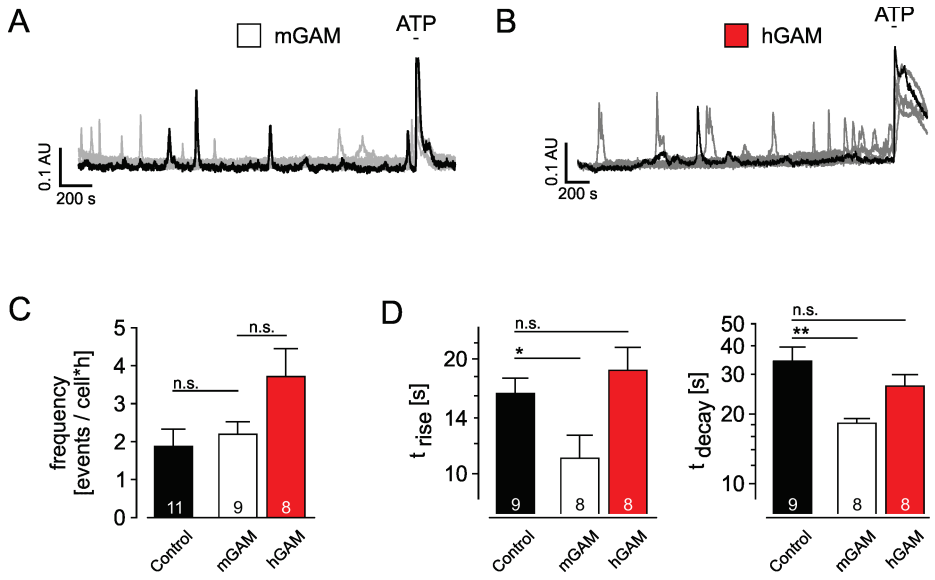

Figure 6. Spontaneous Ca^{2+} transients of Glioma-associated microglia

A-B. Representative traces of experiments on glioma-associated microglia from mouse (A) and human (B). Note that spontaneous Ca^{2+} transients occur in both cell preparations. **C.** Mean frequencies of spontaneous Ca^{2+} transients in freshly isolated control microglia (from data shown in Fig. 1A) and glioma-associated microglia from mouse and human. No significant difference was found between the groups. **D.** Mean of the rise (left) and decay (right) times of spontaneous Ca^{2+} transients of freshly isolated microglia and glioma-associated microglia from mouse and human. The tumor context significantly accelerates the kinetics of spontaneous Ca^{2+} transients in mouse microglia. Numbers on the bars indicate the number of experiments (coverslips).

Supplement

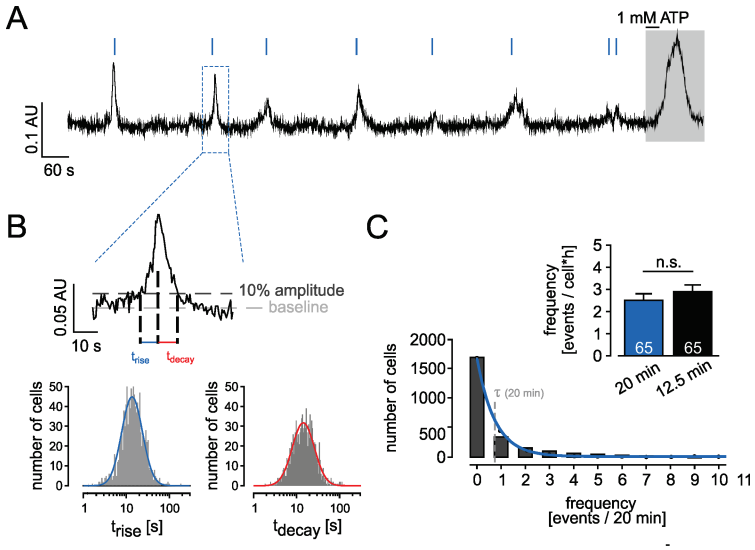

Suppl.Fig.1. Determination of the frequency and kinetics of spontaneous cytosolic Ca^{2+} transients.

A. Sample trace of a fluometric Ca^{2+} recording on a neonatal cultured microglia. Intracellular Ca^{2+} is given as the mean fluorescence within a manually-set ROI over the time. Values are normalised to the fluorescence at the beginning of the experiment (F/F_0). Blue arrows indicate the Ca^{2+} elevations that were taken as spontaneous transients and used for further analysis.

B. Top, magnification of one transient from the trace shown in A. Rise time (t_{rise}) and decay time (t_{decay}) were determined by measuring the time interval between 10% baseline and peak. Bottom. Histograms of t_{rise} and t_{decay} of neonatal microglia under control conditions were normally distributed on a logarithmic scale. A Gauss fit was used to calculate the mean of $\log(t_{rise})$ and $\log(t_{decay})$. All statistical calculations were done with the $\log(t_{rise})$ and $\log(t_{decay})$ values.

C. Histogram of the frequency of spontaneous Ca^{2+} transients in individual microglial cells. The data were fitted with an exponential function. The calculated tau-value of that fit was taken as the average number of events per cell and analysed time interval (20 min in the example shown). For clarity, all frequency data were scaled to events per hour and cell (events/cell*h). The bar graph in the inset shows that the frequency values of transients determined within a 20 min and a 12.5 min recording interval were similar, indicating the values did not dependent on the time window of analysis.

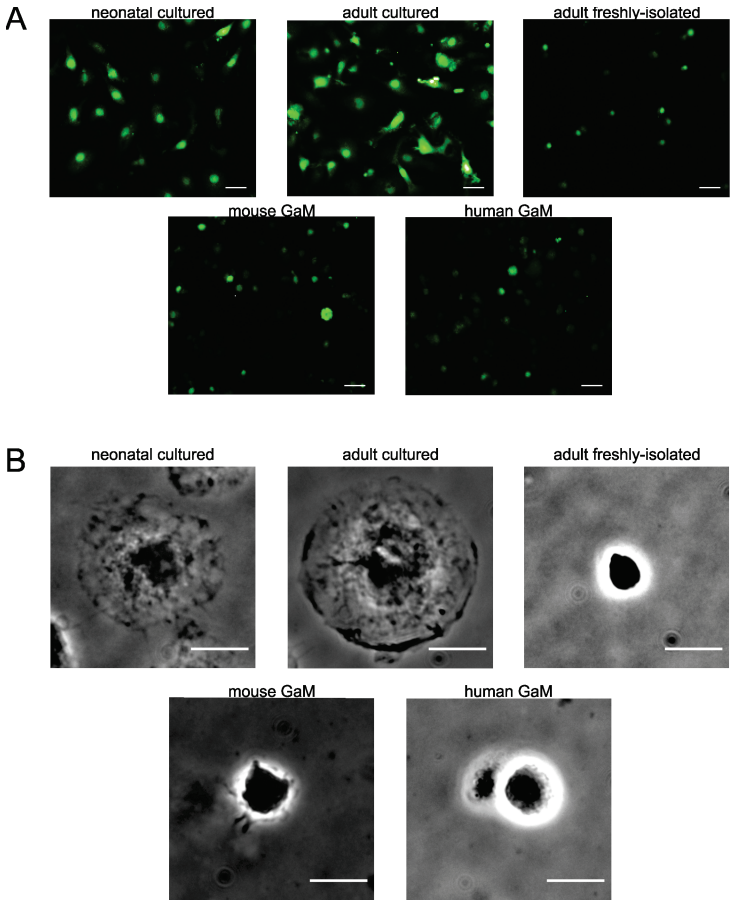

Suppl.Fig.2. Morphology of isolated microglia

A. Sample images of calcium experiments on neonatal and adult cultured, adult freshly-isolated (top row, from left) as well as mouse and human glioma-associated microglia (bottom row). Cells were loaded with the membrane-permeable, Ca^{2+}-sensitive dye Fluo-4. Shown is the maximum-intensity projection of a Ca^{2+} imaging movie that included 15 min of control conditions (standard buffer) and application of 1 mM ATP for 30 s. Scale bar: 20 µm.

B. Phase contrast images of representative microglia (63X, Ph2). Microglial processes were only present after culturing whereas freshly-isolated microglia were devoid of them. Scale bar: 10 µm.

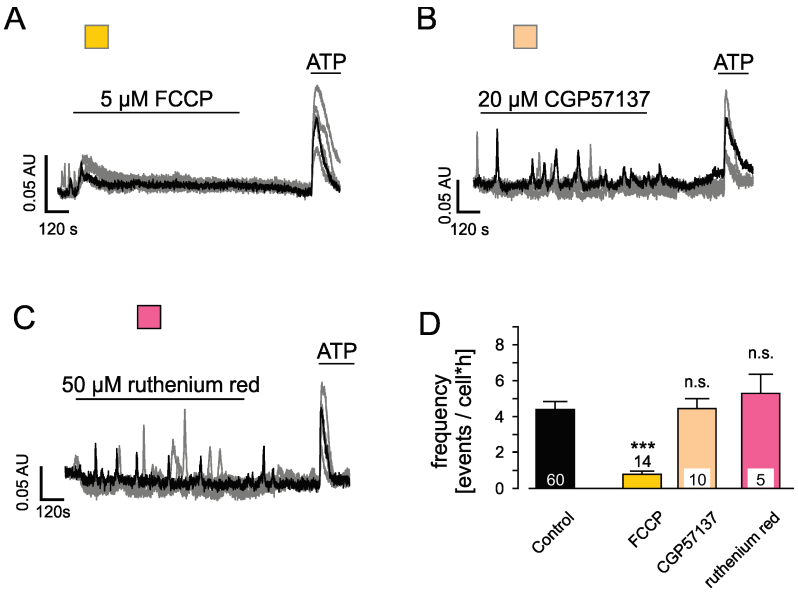

Suppl.Fig.3 Spontaneous Ca^{2+} transients in microglia emerge from ER Ca^{2+} stores.

A. Application of 5 µM FCCP strongly diminishes the frequency of spontaneous Ca^{2+} transients in cultured neonatalmicroglia. Note the transient Ca^{2+} increase shortly after the wash-in of FCCP.

B. Inhibition of the mitochondrial Na^{+}/Ca^{2+} exchanger by CGP57137 (20 µM) had no influence on the occurrence of spontaneous Ca^{2+} transients in microglia.

C. 50 µM ruthenium red (RR), a blocker of N- and P-type Ca^{2+} channels did not impede spontaneous Ca^{2+} transients. RR also blocks Ca^{2+} uptake and release from mitochondria, and Ca^{2+} release from ryanodine-sensitive intracellular stores.

D. Mean frequencies of spontaneous Ca^{2+} transients in neonatal cultured microglia under control conditions (black) and in the presence of 5 µM FCCP, 20 µM CGP57137 or 50 µM ruthenium red. Bars are colored as in A-C. Black bar shows data of neonatal microglia under control conditions (see Fig.1C for sample traces). Statistics: n.s.: not significant; ***: $p<0.001$. Numbers on the bars indicate the number of experiments (coverslips).